# Effect of the Synthesis Method, Complexing Agent and Solvent on the Physicochemical Properties of LaNiO$_3$ Nanopowders

[1]Djani Faiçal*, [2]Arturo Martínez-Arias and [3]Muazzez Gürgan

[1]*Molecular Chemistry Laboratory and Environment, University Mohamed Khider, 07000 Biskra, Algeria.*
[2]*Instituto de Catálisis y Petroleoquímica, CSIC, C/Marie Curie 2,*
*Campus de Cantoblanco, 28049 Madrid, Spain.*
[3]*Department of Biology, Tekirdag Namık Kemal University, 59030 Tekirdag, Turkey.*
f.djani@univ-biskra.dz*

**Summary:** LaNiO$_3$ nanopowders are synthesized by sol–gel and sol-gel combustion methods using citric acid, ascorbic acid and sucrose as chelating agents, and ethanol and water as solvents. The precursor thermal decomposition towards the final solid was analyzed by X-ray diffraction, differential thermal analysis and thermogravimetric techniques which were also used to provide the adequate temperature of calcination (800°C) for achievement of the final perovskite. After calcination, the nanocomposites were characterized by powder size distribution, Fourier transform infrared spectroscopy and X-ray diffraction.

**Keywords**: Perovskite; LaNiO$_3$; Sol-gel; Combustion; Chelating agent; Solvent.

## Introduction

Materials with composition ABO$_3$ with rare earth elements and 3d transition metals in the positions A and B, respectively, are critical perovskite mixed oxides which exhibit impressive catalytic, magnetic, optical and electrical properties [1-4]. Lanthanum Nickel oxide in the form perovskite (LaNiO$_3$) is among most interesting perovskite mixed oxides as it can be used as an electrode material for conversion and storage [7-11], it is active for redox reactions containing CO, NO or soot [12, 13], or as a catalyst for the combustion of volatile organic compounds [14-15], as a consequence of its electronic and catalytic properties. The method of preparation frequently has an effect on the chemical and physical properties of a material and which affect its potential application. For the synthesis of LaNiO$_3$ with various characteristics, different preparative procedures were used. Ceramic process, molten salt method, co-precipitation method, hydrothermal method and the sol-gel technique have been employed in this sense [4]. The sol-gel preparation method has many advantages, such as better control of the structure, including porosity and particle size, high purity, no need for special or expensive equipment, better homogeneity and less energy consumption. In this work, the sol-gel method was chosen to synthesize and examine different preparation parameters (type of solvent or complexing agents as well as reaction temperature) which can affect the properties of LaNiO$_3$. In this regard, in order to prepare different LaNiO$_3$ catalysts, the Pechini approach was utilized as a sol-gel route while sol-gel combustion using citric acid, ascorbic acid and sucrose as chelating agents, and methanol, ethanol and water as solvents were explored.

## Experimental

### Preparation

*Preparation of the oxides LaNiO$_3$ by sol-gel using distilled water and ethanol as solvents*

LaNiO$_3$ was prepared by the sol-gel method using the Pechini approach where citrate was used as complexing agent [16]. La (NO$_3$)$_3$.6H$_2$O (Sigma Aldrich), Ni (NO$_3$)$_3$.6H$_2$O (Sigma Aldrich), Ethanol (99%, Fluka), distilled water (H$_2$O) and citric acid monohydrate (Sigma Aldrich) were used as reagents. The solutions of citric acid and metal nitrates with water and ethanol were made independently and later mixed together and stirred for 5 h. The ethanol was slowly evaporated at 80°C and so the solution was concentrated to obtain a gel which was later dried at 100°C in an oven whose temperature was slowly raised. Then, a solid amorphous citrate precursor was obtained by keeping the temperature constant overnight. The citrate precursor was calcined at 800°C for 5 h in air [17, 18]. The calcination temperature was determined by precursor decomposition analysis under air, as exposed below.

*Preparation of the oxides LaNiO$_3$ by sol-gel employing citric acid, ascorbic acid and sucrose as complexing agents.*

LaNiO$_3$ was prepared using the Pechini approach where citrate was used as complexing agent [16]. La (NO$_3$)$_3$.6H$_2$O (Sigma Aldrich), Ni (NO$_3$)$_3$.6H$_2$O (Sigma Aldrich), distilled water (H$_2$O) and citric acid monohydrate (Sigma Aldrich), ascorbic acid (Fluka) and sucrose (Fluka) were used as reagents. The solutions of

complexing agent and metal nitrates with water and methanol were made independently and later mixed together and stirred for 5 h. The methanol was slowly evaporated at 80ºC and so the solution was concentrated to obtain a gel which was later dried at 100 ºC in an oven whose temperature was slowly raised. This produced a solid amorphous citrate precursor upon keeping the temperature constant overnight. The citrate precursor was calcined at 800ºC for 5 h in air [17, 18]. The calcination temperature was determined by precursor decomposition analysis under air, as shown below.

### Preparation of the oxides LaNiO₃ by sol-gel combustion

$LaNiO_3$ was prepared using the sol-gel combustion method with citrate as the complexing agent [16]. La $(NO_3)_3$.6$H_2O$ (Sigma Aldrich), Ni $(NO_3)_3$.6$H_2O$ (Sigma Aldrich), distilled water ($H_2O$) and citric acid monohydrate (Sigma Aldrich) were used as reagents. The solutions of complexing agent and metal nitrates with water and methanol were made independently and later mixed together and stirred for 1 h. The methanol was slowly evaporated at 80ºC and so the solution was concentrated to obtain a gel which was later heated at 250ºC, at which all precursors were combusted and finally the temperature was decreased to room temperature. The precursor was calcined at 800ºC for 5 h in air [17, 18]. The calcination temperature was determined by precursor decomposition analysis under air, as examined below.

### Characterization

### X-ray diffraction

XRD Patterns were collected on a Bruker AXS D8- advance diffractometer employing Cu Kα radiation. In all diffractograms, a step size of 0.02º (2θ) was used with a data collection time of 15 s. Data were collected between 2θ values of geometry. Identification of crystalline phases was carried out between 10 and 80° using standard θ/2 configuration and by comparison with JCPDS standards. The unit cell parameters were obtained by fitting the peak position of the XRD pattern using the Match and X'pert Highscore programs.

### Infrared spectroscopy

Fourier transform spectrometer (FTIR) (Shimadzu 8400S) was used to obtain infrared transmission spectra which were recorded in the 400-4000 cm⁻¹ range. A granular technique was used with 1 mg of sample added to 200 mg of KBr.

### Thermal characterizations (TGA) of precursors

Thermogravimetric analysis (TGA) of the precursor decomposition was performed on a Perkin-Elmer TGA7 device, respectively, from 20 to 900 ºC at a heating rate of 10 ºC min⁻¹. This analysis aims to determine the temperature of decomposition of the precursors under atmospheric air (after the drying step of the preparation at 100 ºC) in order to decide about calcination conditions required to achieve the desired oxide material.

### Powder size distribution (PSD)

With the aim of determining the effect of the type of complexing agent or solvent employed as well as the synthesis method on the particle size, the distribution of the grain size of the samples was analyzed by laser granulometry. The obtained powder after the calcination was dissolved in deionized water using magnetic stirrer combined with ultrasound for 15 minutes prior to the analysis. Then the powder size distribution was performed by using a laser particle size analyzer (Mastersizer 2000, Malvern).

### Results and Discussion

XRD Patterns obtained for the compounds under study are shown in the following Figs:
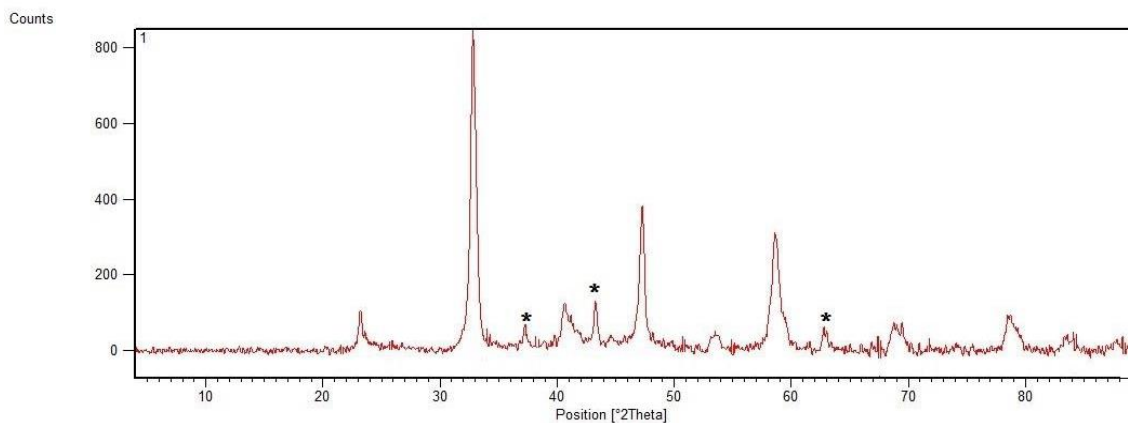


(a)
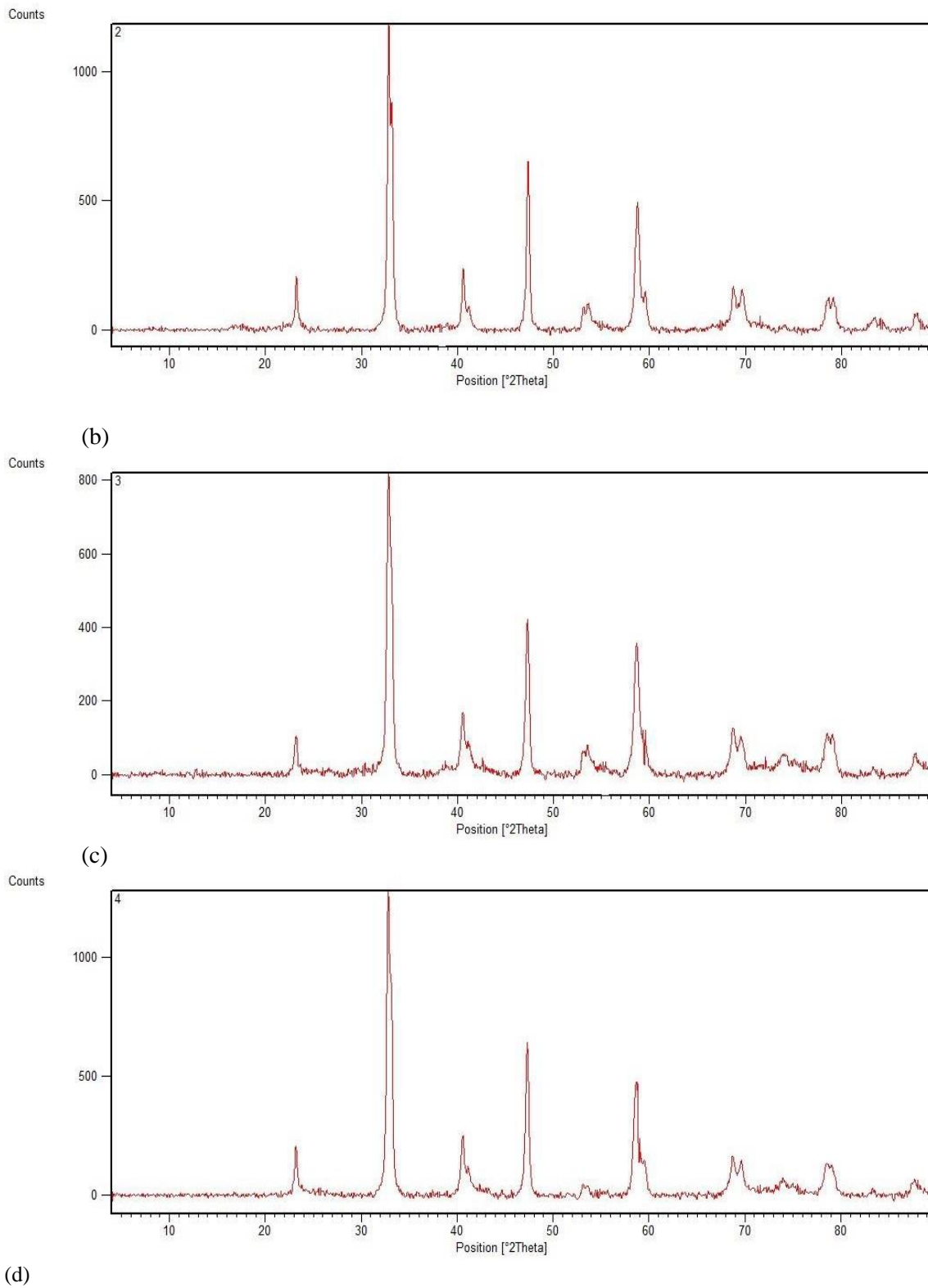
Fig. 1:  XRD patterns of LaNiO$_3$ prepared by sol-gel and calcined at 800 ºC using different solvent or complexing agent: a) sample S1, Water and citric acid, Peaks marked with * correspond to NiO, b) sample S2, ethanol and citric acid, c) sample S3, sucrose and water d) sample S4, ascorbic acid and water.

The observed values of the 2θ with JCPDS standards (00-033-0711) for this type of compound (based on X'pert highscore software) demonstrate the presence of the perovskite phase $LaNiO_3$ in all cases (S1, S2, S3, S4), identified as the perovskite-type phase with rhombohedral symmetry, space group R3m [19, 20, 21]. Additional peaks were shown in the diffractogram of the sample S1 ($LaNiO_3$ prepared by water and citric acid), the most intense ones appearing at 2θ~ 37.2, 43.3 and 62.80 which correspond to cubic NiO (00-047-1049) [19, 22].

XRD patterns of $LaNiO_3$ prepared by sol-gel combustion using water and citric acid, before and after calcination are shown in the following Figs:

As shown in Fig. 2, $LaNiO_3$ prepared by sol-gel combustion requires calcination at 800 °C for 5 hours with a rate of 5°C.min$^{-1}$ in order to form the perovskite phase of rhombohedral symmetry and space group of R3m. The observed peaks are consistent with JCPDS standard for this type of compound (based on X'pert highscore software) and demonstrate the presence of a single phase which is the perovskite $LaNiO_3$ [23, 24].

Infrared spectra of the samples prepared with various complexing agents and different methods of synthesis after calcination are almost identical. Fig 3 shows a characteristic infrared spectrum for the sample prepared by sol-gel using water and citric acid after calcination at 800 °C.



(a)



(b)
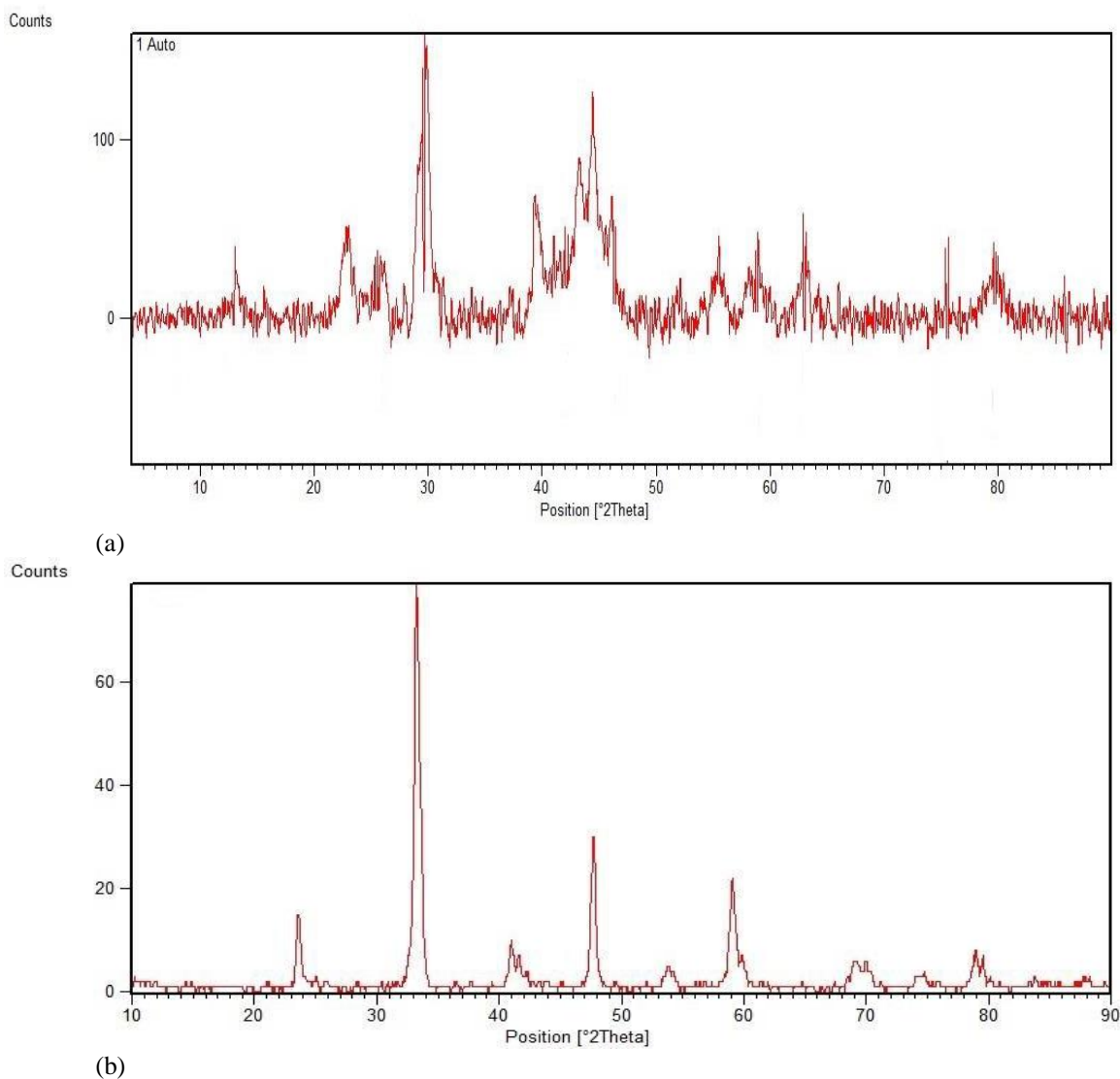
Fig. 2:   XRD patterns of $LaNiO_3$ (S5) prepared by sol-gel combustion using Citric acid and water a) before (precursor after the combustion reaction) and b) after calcination at 800 °C (sample S5).
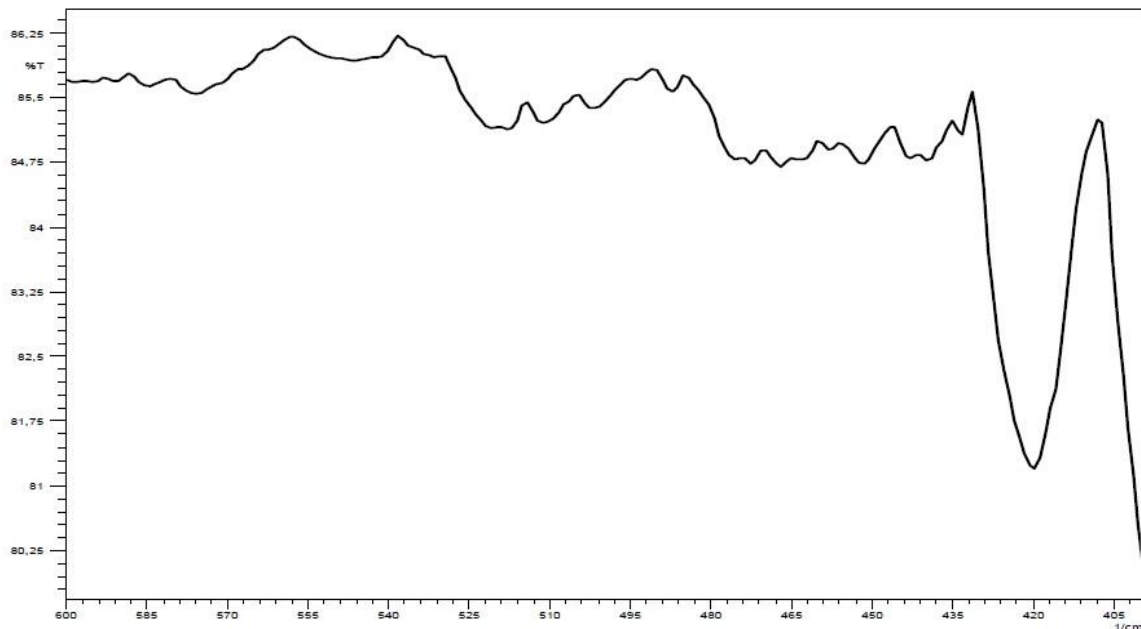
Fig. 3:    Infrared spectrum (400-600 cm$^{-1}$ region) of LaNiO$_3$ prepared by sol-gel using water and citric acid after calcination at 800 °C.

The infrared spectra of these five samples after calcination at 800°C showed strong and well-defined absorption bands, typical of perovskite oxides [25]. Typically, the M-O (M = Ni) vibrations of octahedral MO$_6$ units dominated the spectra. Thus, the infrared spectra showed a band at about 420 cm$^{-1}$ attributed to vibrations of the Ni-O bond in the perovskite LaNiO$_3$ and in contrast to the infrared spectra observed before calcination [26].

TGA results for the xerogel precursors (after the drying step) are displayed in Fig 4:



(b)



(a)
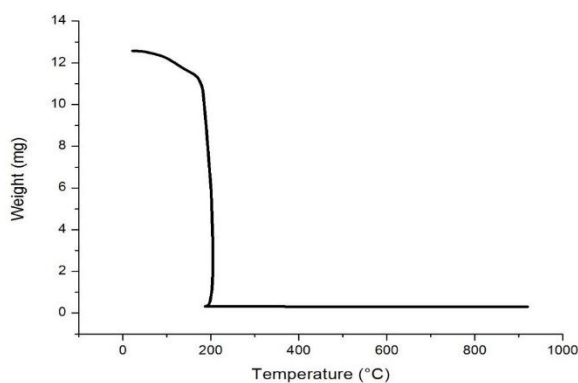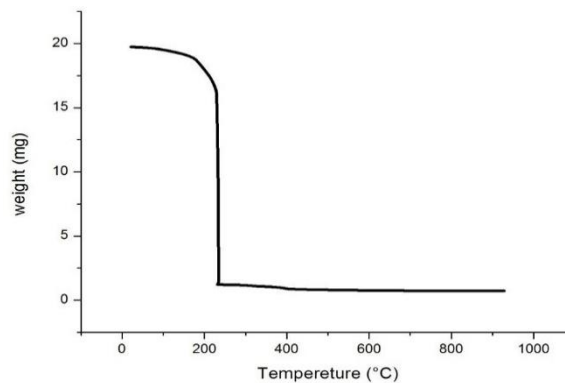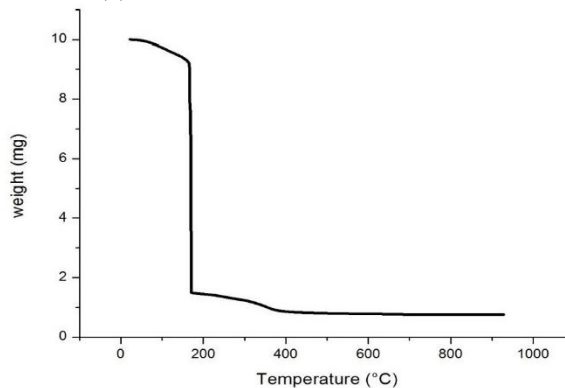


(c)
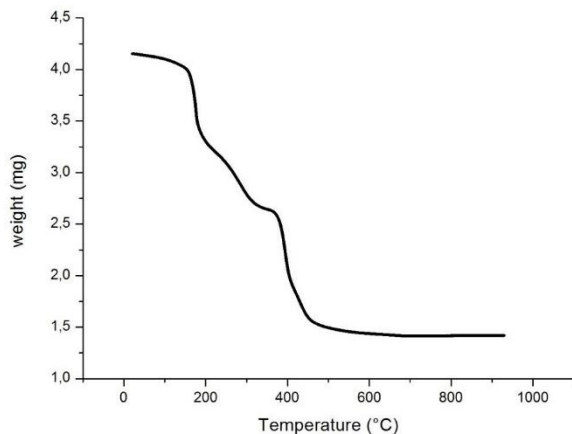
(d)

Fig. 4:    TGA curves during heating under air of the LaNiO₃ precursors (after the drying step) prepared by sol-gel using: a) S1, water and citric acid, b) S2, ethanol and citric acid, c) S3, sucrose and water d) S4, ascorbic acid and water.

When examining the TGA curves for the four samples (S1, S2, S3, and S4) during heating under air, they can be divided into three decomposition processes: The first region, which extends from 25 up to about 200 °C, exhibits a similar weight loss for three of the samples (S1, S2, and S3) ranging between 85 and 95 % In contrast, the weight loss for the fourth sample, S4, was only 5% in that region, which indicates the desorption of adsorbed or hydration water that may remain in the precursors and the sudden charring of citric acid, ascorbic, and sucrose polymer [23, 27, 16, 28]. In the second region, up to 400 °C, weight loss changes between 1 and 30 % correspond to the slow combustion of carbon and the oxidative decomposition of citrates complexing the metals in the precursors [29, 31]. The third and final region, in which all organic complexes are eliminated, begins differently for each sample, with weight loss ranging from 3% to 30% [30]. Changes can occur in the crystal structure in this region, which we call allotropic variables, not necessarily accompanied by weight loss. The results of the thermal analysis show that the weight loss may reach 98 %, and this may be due to the fact that the method of synthesis includes organic compounds with a considerable weight and which, according to this analysis, are only completely removed at relatively high temperatures, which is considered one of the defects in the field.

The analysis of the distribution of the grain size of the samples was employed in order to show the influence of the complexing agent, solvents and the synthetic methods employed on the particle size by laser granulometry. The results are displayed in Fig 5:
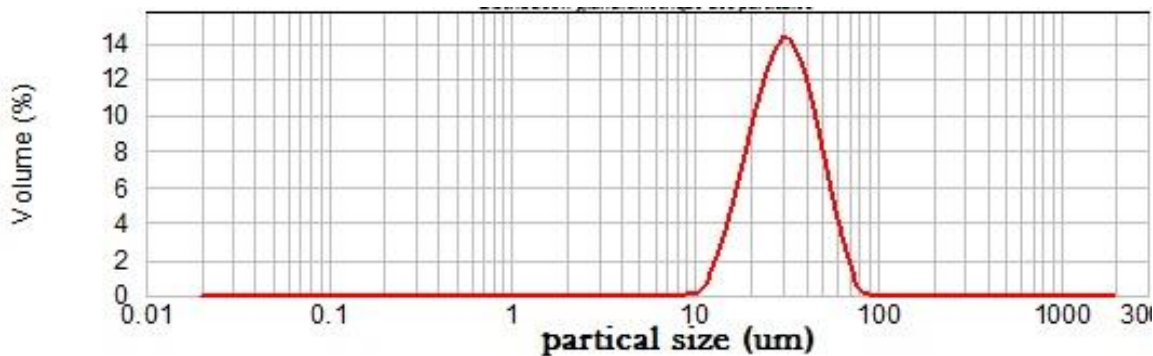


(a)
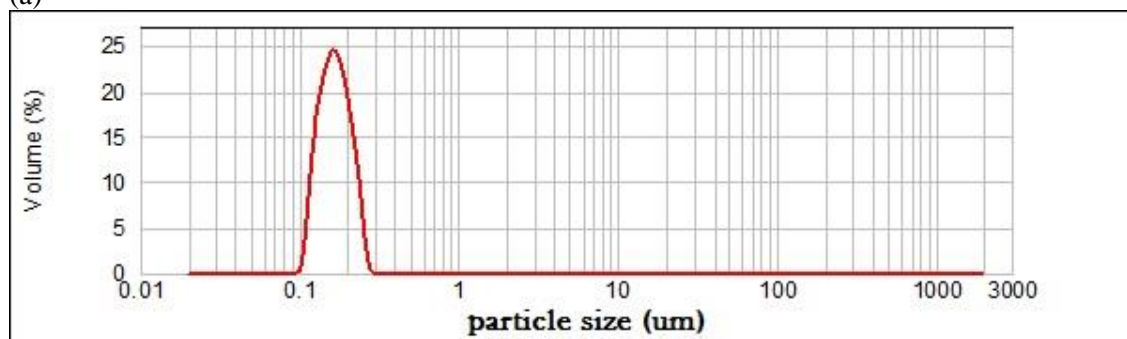


(b)
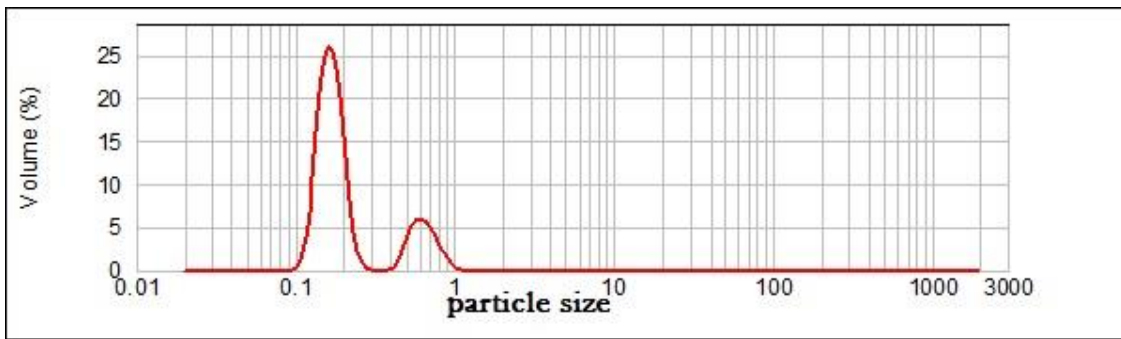
(c)
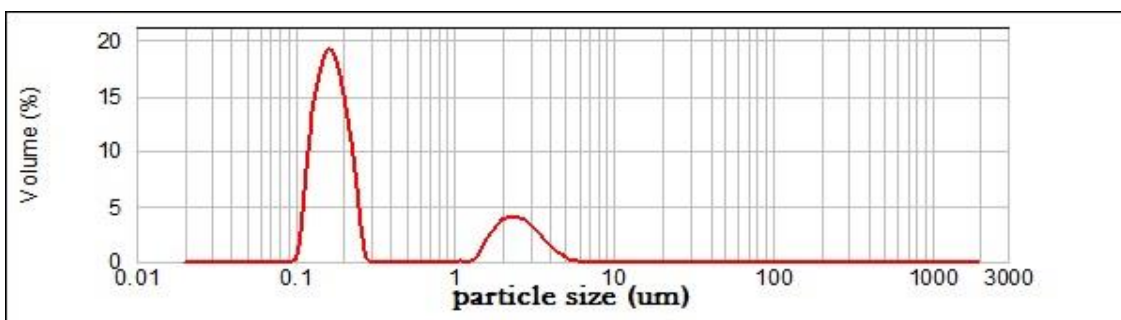
(d)
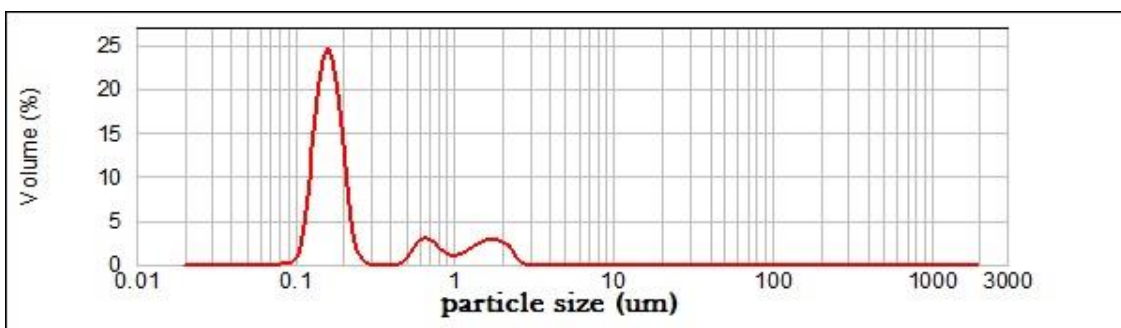
(e)
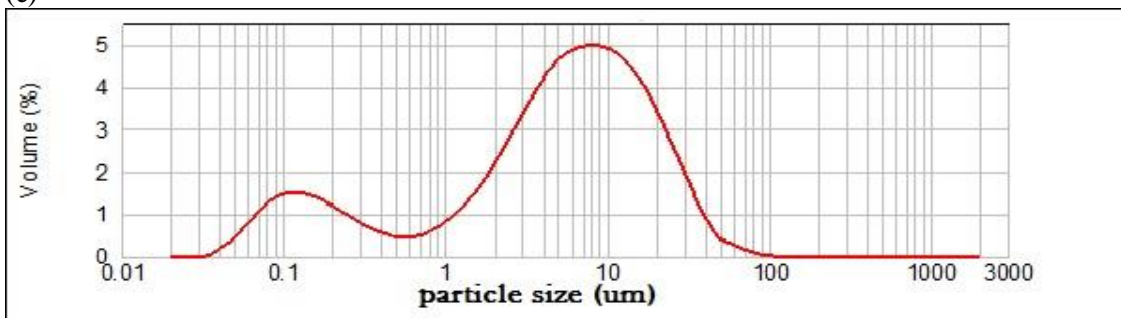
(f)

Fig. 5:   Particle size distribution of LaNiO$_3$ prepared by sol-gel (samples calcined at 800 ºC) using: a) S1, water and citric acid, b) S2, ethanol and citric acid, c) S3, sucrose and water and d) S4, ascorbic acid and water. Sample S5 prepared by sol-gel combustion using citric acid and water e) before and f) after calcination at 800 ºC.

Table-1: Particle size of the samples prepared by different complexing agent, solvents and the synthetic methods.

| sample | S.M | C.A | S | particle size (µm) | | | volume % | | |
|--------|-----|-----|---|-----|-----|-----|-----|-----|-----|
| S1 | S.G | ci.a | w | 12.5 | - | - | 15 | - | - |
| S2 | S.G | ci.a | eth | 0.159 | - | - | 25 | - | - |
| S3 | S.G | suc | w | 0.159 | 0.58 | - | 26 | 6 | - |
| S4 | S.G | as.a | w | 0.159 | 2.244 | - | 19 | 4 | - |
| S5 before cal | S.G.C | ci.a | w | 0.159 | 0.630 | 1.589 | 25 | 2.27 | 2.16 |
| S5 after cal | S.G.C | ci.a | w | 0.112 | 7.096 | - | 1.6 | 5 | - |

Unimodal particle size distribution of samples S1 and S2 is observed, in which the peak is centered at 30 microns and 159 nm with volume distribution of 15 and 25 %, respectively. As for the other samples, we note the presence of bimodal particle size distribution. Thus, for sample S3, the first mode consists of a peak centered at 0.159 microns with volume distribution is 26%, and is followed by a second mode with 6% of the distribution whose mean particle diameter is 0.580 microns. Concerning sample S4, the first mode is centered at 0.159 microns with volume distribution of 19%, and is followed by the second mode with 4% of the distribution whose mean particle diameter is 2.244 microns. Sample S5 (before calcination)exhibits three modes of particle distribution, the first of which has a peak centered at 0.159 microns whose volume distribution is 25%, followed by a second mode of 2.27 percent of the distribution with a particle diameter of 0.630 microns, and a third mode at 1.589 microns and V= 2.16 %. Finally, sample S5 (after calcination) has two modes of particle distribution, the first mode of which is related to a peak centered at 0.112 microns whose volume distribution is 1.6%, and is followed by a second mode with 5% of the distribution whose particle diameter is 7.096 microns.

The following Table 1 represents the particle size of the samples prepared by different complexing agent, solvents or synthetic method:

*S.M: synthesis method, S.G: sol gel, S.G.C: sol gel combustion; C.A: complexing agent, ci.a: citric acid; suc: sucrose; as.a: ascorbic acid; S: solvent, w: water, eth: ethanol.*

It is noted that the particle size of the sample prepared by citric acid with ethanol as solvent (0.159 µm) is similar than that prepared by using sucrose or ascorbic acid as complexing agents while the particle size of LaNiO$_3$ prepared by sol-gel combustion (after calcination) is lower than that synthesized by citric acid in water (12.5 µm).

The most homogeneous distribution is that of the sample prepared by citric acid in ethanol, in which unimodal distribution is detected with mean diameter of 159 nm. Not to mention the effect of dispersant and the effect of crushing, a reltively small particle size is obtained upon using the sol-gel method (after calcination) and in any case the best homogeneity is that of sample prepared by sol-gel method (citric acid - ethanol) for which 159 nm size is detected [32].

## Conclusions

In this work we have synthesized the perovskite LaNiO$_3$ using two methods: sol-gel and sol-gel combustion with two solvents (ethanol and water), and different complexing agents. Physicochemical characterization of the system LaNiO$_3$ have brought us to the following conclusions:

1. The study by X-ray diffraction, has allowed us to identify the phase of LaNiO$_3$ system at the selected temperature of calcination (800 ºC). In turn, it evidences that the oxides have a perovskite structure with rhombohedral symmetry and space group R3m.
2. The analysis by laser particle size has allowed us to follow the evolution of the particle size of the oxide LaNiO$_3$ which exhibits different distribution as a function of preparation parameters employed in each case.
3. Thermogravimetric analysis (TGA) allowed us to identify different transformations that take place during the thermal treatment of the precursors under air and the corresponding calcination temperatures required to convert the hydroxide form of the various metals to the oxide form, which starts from 500 ° C as well as it allowed determining the stability range of the pure perovskite phase in the temperature range studied.
4. Infrared spectra (IR) of the oxide LaNiO$_3$ show that the bands related to the hydroxide group and water and (C=O) have disappeared completely after calcination at 800 ºC. The intense band observed at 420 cm$^{-1}$ corresponds to the stretching vibration which indicates the formation of the Ni-O band in all samples and evidences that the oxide LaNiO$_3$ becomes developed in both solvents (ethanol-water) and upon use of different agents of complexation or synthesis method.

## References

1. L. Ph, J. B. Torrance, J. S. A. I. Pannetier, A. I. Nazzal, P. W. Wang, and T. C. Huang, Synthesis, crystal structure, and properties of metallic $PrNiO_3$: Comparison with metallic $NdNiO_3$ and semiconducting $SmNiO_3$, *J. Solid State Chem.*, **91**, 225 (1991).

2. C. M. Sen, T. B. Wu, and J.M. Wu, Effect of textured $LaNiO_3$ electrode on the fatigue improvement of $Pb(Zr_{0.53}Ti_{0.47})O_3$ thin films, *Appl Phys Lett*, **68**, 1430 (1996).

3. R. N. Singh, S. K. Tiwari, S. P. Singh, A. N. Jain, N. K. Singh, Electrocatalytic activity of high specific surface area perovskite-type $LaNiO_3$ via sol-gel route for electrolytic oxygen evolution in alkaline solution, *Int J Hydrogen Energ*, **22**, 557, (1997).

4. M. A. Peña, J. L. G. Fierro, Chemical structures and performance of perovskite oxides, *Chem. Rev.*, **101**, 1981, (2001).

5. L. T. Rong, Z. B. Chen, and M.D. Lee, Catalytic behavior and electrical conductivity of $LaNiO_3$ in ethanol oxidation, *Appl. Catal., A*, **136**, 191, (1996).

6. B. Martin, M. Pirjamali, and Y. Kiros, $La_{0.6}Ca_{0.4}CoO_3$, $La_{0.1}Ca_{0.9}MnO_3$ and $LaNiO_3$ as bifunctional oxygen electrodes, *Electrochim. Acta*, **47**, 1651, (2002).

7. S. M. Lima, J. M. Assaf, M. A. Peña, J. L. G. Fierro, Structural features of $La_{1-x}Ce_xNiO_3$ mixed oxides and performance for the dry reforming of methane, *Appl. Catal., A*, **311**, 94 (2006).

8. V. Gustavo, A. Kiennemann, and M. R. Goldwasser, Dry reforming of $CH_4$ over solid solutions of $LaNi_{1-x}Co_xO_3$, *Catal. Today*, **133**, 142, (2008).

9. V. Gustavo, M. R. Goldwasser, C. U. de Navarro, J. M. Tatibouet, J. Barrault, C. B. Dupeyrat, and F. Martínez, Dry reforming of methane over Ni perovskite type oxides, Catal. Today, **107**, 785 (2005).

10. S. M. de Lima, A. M. da Silva, L. O. O. da Costa, J. M. Assaf, G. Jacobs, B. H. Davis, L. V. Mattos, F. B. Noronha, Evaluation of the performance of $Ni/La_2O_3$ catalyst prepared from $LaNiO_3$ perovskite-type oxides for the production of hydrogen through steam reforming and oxidative steam reforming of ethanol *Appl. Catal., A*, **377**, 181, (2010).

11. P. Rosa, V. M. Gonzalez-dela Cruz, A. Caballero, and J. P. Holgado, $LaNiO_3$ as a precursor of $Ni/La_2O_3$ for $CO_2$ reforming of $CH_4$: Effect of the presence of an amorphous NiO phase, *Appl. Catal., B*, **123**, 324, (2012).

12. A. K. Norman, M. A. Morris, The preparation of the single-phase perovskite $LaNiO_3$, *J Mater Process Tech*, **92**, 91 (1999).

13. N. Russo, D. Fino, G. Saracco, V. Specchia, Promotion effect of Au on perovskite catalysts for the regeneration of diesel particulate filters, *Catal. Today*, **137**, 306, (2008).

14. G. Pecchi, P. Reyes, R. Zamora, L. E. Cadús, J. L. G. Fierro, Surface properties and performance for VOCs combustion of $LaFe_{1-y}Ni_yO_3$ perovskite oxides, *J. Solid State Chem.*, **181**, 905, (2008).

15. R.M. Garcıa de la Cruz, H. Falcon, M. A. Pena, and J. L. G. Fierro, Role of bulk and surface structures of $La_{1-x}Sr_xNiO_3$ perovskite-type oxides in methane combustion, *Appl. Catal., B*, **33**, 45, (2001).

16. N. T. Hong Le, J. M. Calderón-Moreno, M. Popa, D. Crespo, and N. X. Phuc, $LaNiO_3$ nanopowder prepared by an 'amorphous citrate' route, *J Eur Ceram Soc.*, **26**, 403, (2006).

17. N. A. Merino, B. P. Barbero, P. Grange, L, E. Cadús, $La_{1-x}Ca_xCoO_3$ perovskite-type oxides: preparation, characterisation, stability, and catalytic potentiality for the total oxidation of propane, *J. Catal.*, **231**, 232, (2005).

18. R. Z. Yarbay, H. E. Figen, and S. Z. Baykara, Effects of Cobalt and Nickel Substitution on Physical Properties of Perovskite Type Oxides Prepared by the Sol-Gel Citrate Method, *Acta Phys Pol A,* 121, 44, (2012).

19. N. S. Gonçalves, J. A. Carvalho, Z. M. Lima, and J. M. Sasaki, Size–strain study of NiO nanoparticles by X-ray powder diffraction line broadening, *Mater Lett.*, **72**, 36 (2012).

20. E. Bontempi, C. Garzella, S. Valetti, L. E. Depero, Structural study of $LaNi_xFe_{1-x}O_3$ prepared from precursor salts, *J Eur Ceram Soc.*, 23, 2135 (2003).

21. P. Erri, P. Dinka, A. Varma, Novel perovskite-based catalysts for autothermal JP-8 fuel reforming, *Fuel Cell Bull*, **2006**, 12, (2006).

22. T. Ohzeki, T. Hashimoto, K. Shozugawa and M. Matsuo, Preparation of $LaNi_{1-x}Fe_xO_3$ single phase and characterization of their phase transition behaviors, *Solid State Ion*, **181**, 1771 (2010).

23. K. Rida, M. A. Peña, E. Sastre, and A. Martinez-Arias, Effect of calcination temperature on structural properties and catalytic activity in oxidation reactions of $LaNiO_3$ perovskite prepared by Pechini method, *J Rare Earth*, **30**, 210, (2012).

24. M. Kuras, R. Roucou, and C. Petit, Studies of $LaNiO_3$ used as a precursor for catalytic carbon nanotubes growth, *J Mol Cata A Chem*, **265**, 209, (2007).

25. A. E. Lavat, and E. J. Baran, IR-spectroscopic characterization of $A_2BB'O_6$ perovskites, *Vib Spectrosc.*, **32**, 167, (2003).

26. W. Zheng, R. Liu, D. Peng, and G. Meng, Hydrothermal synthesis of $LaFeO_3$ under carbonate-containing medium, *Mater Lett.*, **43**, 19, (2000).

27. P. S. Devi, and M. S. Rao, Study of the thermal decomposition of lanthanum and chromium citrate hydrates, *J Anal Appl Pyrol.*, **22**, 187, (1992).

28. H. Wang, Y. Zhu, P. Liu and W. Yao, Preparation of nanosized perovskite $LaNiO_3$ powder via amorphous heteronuclear complex precursor, *J. Mater. Sci.*, **38**, 1939, (2003).

29. M. Biswas, Synthesis of single phase rhombohedral $LaNiO_3$ at low temperature and its characterization, *J Alloy Compd.*, **480**, 942, (2009).

30. F. S. Oliveira, P. M. Pimentel, R. M. P. B. Oliveira, D. M. A. Melo, and M. A. F. Melo, Effect of lanthanum replacement by strontium in lanthanum nickelate crystals synthetized using gelatin as organic precursor, *Mater Lett.*, **64**, 2700, (2010).

31. J. D. G. Fernandes, D. M. A. Melo, A. M. G. Pedrosa, M. J. B. Souza, D. K. S. Gomes, and A. S. Araujo, Synthesis and catalytic properties of lanthanum nickelate perovskite materials, *React Kinet Catal L.*, **84**, 3(2005).

32. F. Djani, M. Omari, A. M. Arias, Synthesis, characterization and catalytic properties of La(Ni, Fe)$O_3$–NiO nanocomposites, *J Sol-Gel Sci Technol*, **78**, 1, (2016).